# APPLICATION OF CONTROL THEORY TO TURBULENCE

Parviz Moin and Thomas Bewley
Department of Mechanical Engineering
Stanford University
Stanford, CA USA

#### **ABSTRACT**

Efficient feedback control laws based on optimal control theory for wall-bounded turbulent flows are discussed. The technique described is unique from the standpoint that it is mathematically based solely on the control objective, the equations governing the fluid flow, and instantaneous observations of the flow, without the adhoc procedures normally used to accomplish flow control.

Two formulations are discussed in detail: the regulation of drag and the terminal control of turbulent kinetic energy. Both schemes have been implemented computationally in their optimal form and are quite efficient for their designed purpose, though the algorithm itself is computationally intensive. Drag reduction of over 50% has been obtained using small amounts of wall transpiration in a low Reynolds number flow, which is over twice what could be obtained via ad hoc control rules in the same flow. Methods to reduce these optimal calculations to practical, yet still optimally based, control rules are discussed.

# INTRODUCTION

Our burgeoning understanding of turbulence has, to date, only been used in ad hoc manners in attempts to control this widespread phenomenon. Efforts to inhibit or enhance observed turbulence phenomena have been limited to large-scale devices and shape modifications. Though the mathematical framework for the control of systems governed by partial differential equations has been established for some time (Lions 1968), attention has focused on applying this theory to turbulence only recently (Abergel and Temam 1990).

The motivation for the formulation and computer simulation of optimal control problems in turbulence is clear—the solutions to such problems will give us new insight into the turbulence phenomena responsible for flow characteristics important in engineering designs, such as drag and heat transfer, and how these phenomena are most effectively altered with small control forces. Such simulations can only be performed on large supercomputers with complete knowledge of the flow, which will put real-time solution of optimal control problems out of reach of laboratory experiments for a long time to come. In light of this. various methods are currently under investigation to assimilate the data gathered by optimal control calculations to reduce them to practical feedback control rules which can be used in laboratory and, eventually, viable commercial implementations.

Reviews of recent progress in the broad field of turbulence control include: Blackwelder (1989), Bushnell and McGinley (1989), Gad-el-Hak (1989, 1994), Fiedler and Fernholz (1990), and Moin and Bewley (1994)—for comprehensive reviews of this subject from a variety of viewpoints, the reader is referred to these references. This article will instead focus on the work of the authors in the application of optimal control theory to the Navier-Stokes equations in order to cast practical turbulence control problems in a rigorous setting, and will survey other approaches in this field only to the extent necessary to put the current work in context.

Active control schemes refer to methods which add energy to a flow, such as unsteady wall transpiration or the prescribed motion of an actuator. These are in contrast to passive techniques, which modify a flow without unsteady external input. Passive techniques include the placement of longitudinal grooves (riblets) on a surface to reduce the drag caused by turbulence (Bechert and Bartenwerfer 1989, Walsh 1990, Choi et al. 1993) and the use of compliant walls which deform in response to the overlying flow to stabilize a laminar boundary layer (Riley et al. 1988).

The external energy added in an active control scheme may be determined in advance (in which case the control scheme is termed open-loop or feedforward) or coordinated with real-time measurements of the flow itself (termed closed-loop or feedback control). The periodic forcing of a round jet (Lee and Reynolds 1985) to produce bifurcation (splitting into two jets) or blooming (expansion to a wide spray of vortex rings) and the hydrodynamic Lorenz forcing of an electrolytic fluid (Nosenchuck and Brown 1993) to restructure flow perturbations in the near wall region are examples of effective open-loop control configurations in turbulent flows. However, in cases in which the control must interact with a specific set of turbulent fluctuations already present in the flow, such as the coherent structures, the random aspect of these structures reduces the effectiveness of an open-loop configuration. In these cases, we seek a "feedback control rule" to relate measurements of the state of the turbulence in the flow to the resulting distribution in space and time of the control energy. The determination of the most suitable mathematical relation between what is sensed and what control is applied will be discussed in this paper.

Large-scale flow management schemes, which sense the gross flow features and then alter fixed or slowly-varying set points of the flow (e.g., the air-fuel ratio in a combustor) in order to optimize some combination of parameters, are well developed. One such example is combustion optimization (Padmanabhan et al. 1993), where the parameters for various open-loop actuators (e.g. speakers and vortex generating jets) are slowly altered using a robust optimization algorithm to simultaneously minimize rms pressure fluctuations and maximize volumetric heat release. It is the subject of the present work to attack a technologically more challenging problem: small scale manipulation of turbulent fluctuations themselves.

#### THE TARGET—TURBULENT STRUCTURES

Coherent motions in turbulent flows (Cantwell 1981, Robinson 1991) provide physical targets for active turbulence control schemes. Through feedback, control effort may be coordinated to manipulate these structures. As the energy of these large-scale structures generally feed the smaller scales of the turbulence spectrum, this can have a

profound overall effect on the turbulence. Herein lies the physical challenge of feedback turbulence control: in the midst of the vast range of spatial and temporal fluctuations of turbulence, identify those unstable coherent structures responsible for the regeneration of the turbulence and the most efficient distribution of control energy to achieve a desired effect.

As a specific example, figure 1 illustrates that high skin friction regions on the wall are often associated with the downward moving side of strong streamwise vortices near the wall. Presumably, by reducing the number or intensity of these nearwall streamwise vortices, one could reduce their tendency to produce such high drag "streaks", and the overall drag might be reduced.

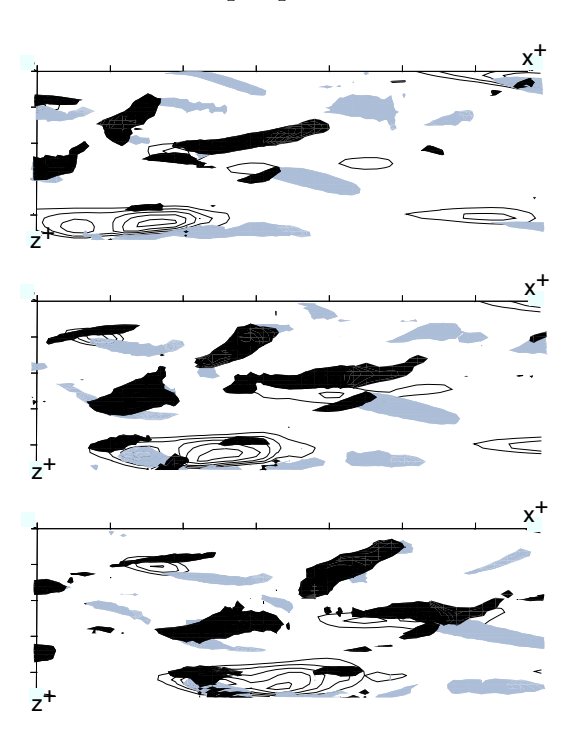


Figure 1: TIME SEQUENCE OF NEAR WALL STRUCTURES (top view). Contour lines indicate skin-friction on the wall. Gray and black regions indicate isosurfaces of negative and positive streamwise vorticity above the wall. Flow is from left to right. From Kravchenko *et al.* (1993).

In situations in which the dominant physics is well understood, such as that shown in figure 1, judgment can guide an engineer to design effective control schemes. An active cancellation scheme motivated by this understanding was used by Choi et al. (1994) to reduce the drag in a fully-developed turbulent flow. By opposing the near-wall motions of the fluid, which often are caused by these near-wall vortices, with an opposing wall control as shown in figure 2, the high

shear region was lifted away from the wall. A direct numerical simulation of this scheme applied to turbulent channel flow demonstrated a maximum of about 20 percent drag reduction when the control was chosen to oppose the vertical motion at  $y^+ = 10$ . Using a Taylor series extrapolation of the velocity gradients at the wall and the equation of continuity to reduce this scheme to a feedback rule relating control velocity to skin friction measurements at the wall alone led only to 6 percent drag reduction. The desire for better performance motivated us to explore more rigorous ways to determine effective feedback control rules.

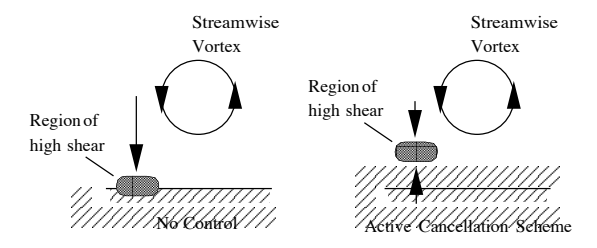


Figure 2: ACTIVE CANCELLATION SCHEME applied to turbulent flow, from Choi et al. (1994).

#### **OPTIMAL CONTROL SCHEMES**

Application of optimal control theory directly to the equations of motion governing the flow, the Navier-Stokes equations, provides a systematic, though (sometimes) very computationally intensive, method for deriving the most efficient distribution of control effort to achieve a desired effect over a finite time interval. In general, as the time interval under consideration T is made larger, the control problem becomes more realistic (and the resulting control becomes more effective), but the optimization problem becomes harder to solve.

The seminal idea of the optimal control method is the iterative minimization of a cost functional which represents the physical problem of interest over a finite time interval, which is taken here without loss of generality to be  $t \in [0,T]$ . Minimization of this functional is achieved by computing the gradient of the cost functional in the space of the control through an adjoint formulation, then updating the control with a gradient algorithm. For an unsteady problem such as turbulence, the cost functional may either be a time-averaged quantity, in which case the control is said to "regulate" this quantity, or an evaluation of the state at the end of the time interval. which is referred to as a "terminal" controller. An unsteady control is to be found on  $t \in (0,T]$ which minimizes the given cost functional.

We shall now consider two examples from Bewley (1996) to illustrate how to apply this method. The first example is the regulation of drag, which is one of the prime motivations for looking at the optimal control method in the first place. The second example is the terminal control of turbulent kinetic energy (TKE), which is done in an attempt to relaminarize low Reynolds number turbulent flows. Note that in the former case a time-averaged flow quantity is important, but in the latter case only the TKE at the end of each optimization interval is important, and thus the latter scheme attempts to relaminarize the flow in stages, allowing high TKE early in each interval without penalty. Studies at low Reynolds number for moderate values of T indicate that the latter approach can actually be more effective at reducing the drag after several optimization intervals, as will be shown.

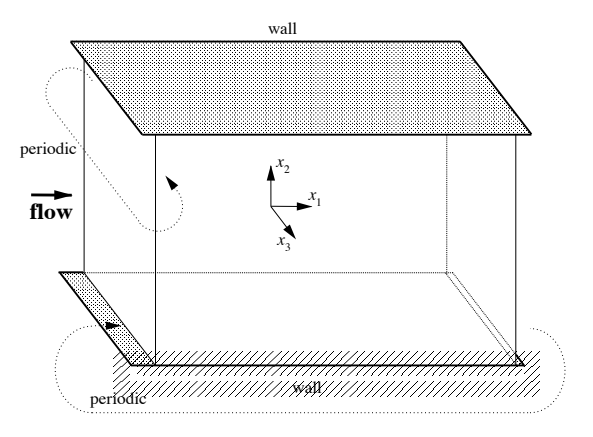


Figure 3: FLOW CONFIGURATION. Blowing and suction is applied through closely spaced holes drilled in the walls to control the flow.

The flow problem we will consider in these examples is turbulent channel flow with no-slip walls and wall-normal control velocities  $\Phi$ . Though this is an idealized geometry, it will give insight into the turbulent behavior which can later be exploited in more practical configurations. This problem is governed by the unsteady, incompressible Navier-Stokes equation and the continuity equation inside the domain  $\Omega$  and normal velocity boundary conditions on the walls w (periodic conditions are implied on the remainder of the boundary of the domain  $\Gamma$ ). This may be written functionally as

$$\mathcal{N}(U) = 0, \tag{1a}$$

with boundary conditions

$$u_i = \Phi n_i$$
 on walls (1b)

and prescribed initial conditions

$$u_i = u_i(0) \qquad \text{at } t = 0. \tag{1c}$$

In the following discussion,  $x_1$  is the streamwise direction,  $x_2$  is the wall-normal direction,  $x_3$  is

the spanwise direction, the  $u_i$ 's are the corresponding velocities, p is the pressure,  $\rho$  is the density, Re is the Reynolds number,  $\delta$  is the channel half-width, and n is a wall-normal unit vector directed *into* the channel, as illustrated in Figure 3. For simplicity, all differential equations will be written in operator form in this discussion—these operators are written out fully in the Appendix.

In this problem, we will be interested in the perturbation  $\dot{U}$  to the flow U resulting from small perturbations  $\dot{\Phi}$  to the control  $\Phi$ . The equation governing this perturbation field may be found by taking the Fréchet differential of the state equation (1) with respect to the control  $\Phi$  (for precise definition of this differential, see Appendix), which may be written

$$\mathcal{A}\dot{U} = 0, \tag{2a}$$

with boundary conditions

$$\dot{u}_i = \dot{\Phi} n_i$$
 on walls (2b)

and initial conditions

$$\dot{u}_i = 0 \qquad \text{at } t = 0. \tag{2c}$$

#### Drag reduction example

As described above, the first step in solving an optimal control problem is to represent the control problem of interest as a cost functional,  $\mathcal{J}$ , to be minimized. In the present problem, control is to be applied to minimize the drag averaged over a section of wall with area A and over the time period [0,T] using the least amount of control effort possible. A relevant cost functional for the present problem is thus

$$\mathcal{J}_d(\Phi) = \frac{1}{AT} \int_{w} \int_0^T \left( \frac{\ell}{2} \Phi^2 + \mu \frac{\partial u_1}{\partial n} \right) dt dS.$$

The first term in the integral is a measure of the magnitude of the control. The second term is a measure of exactly that quantity we would like to regulate—in this case, the drag. These quantities are integrated over the wall section under consideration, of area A, and over the time period under consideration, of duration T. Finally, they are weighted together with a factor  $\ell$ , which represents the price of the control. This quantity is small if the control is "cheap" (which reduces the significance of the first term), and large if applying control is "expensive".

As suggested by Abergel and Temam (1990), a procedure may now be developed to efficiently determine the sensitivity of the cost functional  $\mathcal{J}_d$  to small modifications of the control  $\Phi$ . To do this, we consider the differential to the cost functional  $\mathcal{J}_d$ , and then re-express this differential as a function of the solution to an adjoint problem. The adjoint problem has complexity similar to that of the Navier-Stokes problem (1) governing the state U itself—once it is solved, the gradient direction

 $\mathcal{D}J_d(\Phi)/\mathcal{D}\Phi$  may be easily determined, and thus the control may be updated on (0,T] in the direction that most effectively reduces the cost functional. The flow resulting from this modified control is then recomputed, and the iteration process is repeated until convergence. At this point, the flow is advanced over the entire interval, or a subset thereof, and the iteration process begins anew.

The differential change in the cost  $\dot{\mathcal{J}}_d$  resulting from a differential change of the control  $\dot{\Phi}$  is given by

$$\dot{\mathcal{J}}_d(\Phi) = \frac{1}{AT} \int_w \int_0^T \frac{\mathscr{D} \mathcal{J}_d(\Phi)}{\mathscr{D} \Phi} \dot{\Phi} \, dt \, dS 
= \frac{1}{AT} \int_w \int_0^T \left( \ell \, \Phi \, \dot{\Phi} + \mu \, \frac{\partial \dot{u}_1}{\partial n} \right) \, dt \, dS,$$

where  $\dot{u}_1$  is the first component of the differential state described by (2). Adjoint calculus is used simply to re-express the last term on the right hand side as a linear function of  $\dot{\Phi}$ . Once this is accomplished,  $\dot{\Phi}$  is factored out of the integrand and, as the equation holds for arbitrary  $\dot{\Phi}$ , an expression for the gradient  $\mathcal{D}J_d(\Phi)/\mathcal{D}\Phi$  is extracted

Consider an adjoint state defined by

$$\mathcal{A}^* \tilde{U} = 0, \tag{3a}$$

with boundary conditions

$$\tilde{u}_i = \delta_{i1}$$
 on walls (3b)

and initial conditions

$$\tilde{u}_i = 0$$
 at  $t = T$ , (3c)

where the adjoint operator  $\mathcal{A}^*$  is defined by the identity

$$\langle \mathcal{A}\dot{U}, \tilde{U} \rangle = \langle \dot{U}, \mathcal{A}^*\tilde{U} \rangle + b$$
 (4)

as discussed in the Appendix. Equation (4) may be simplified using (1), (2), and (3). The resulting expression reduces to

$$\int_{w} \int_{0}^{T} \mu \, \frac{\partial \dot{u}_{1}}{\partial n} \, dt \, dS = - \int_{w} \int_{0}^{T} \tilde{p} \, \dot{\Phi} \, dt \, dS.$$

The differential of the cost functional  $\dot{\mathcal{J}}_d$  may be rewritten using this expression, which results in

$$\int_{w} \int_{0}^{1} \left( \frac{\mathscr{D} \mathcal{J}_{d}(\Phi)}{\mathscr{D} \Phi} - \ell \Phi + \tilde{p} \right) \dot{\Phi} \, dt \, dS = 0.$$

As  $\dot{\Phi}$  is arbitrary, this implies that

$$\frac{\mathscr{D}\mathcal{J}_d(\Phi)}{\mathscr{D}\Phi} = \ell \Phi - \tilde{p}.$$

Thus, the sensitivity of the cost functional  $\mathcal{J}_d$  to small changes in the control  $\Phi$  may be determined using the solution to the adjoint problem (3). A control strategy using a simple gradient algorithm may now be proposed such that

$$\Phi^k = \Phi^{k-1} - \alpha \, \frac{\mathcal{D} \mathcal{J}_d(\Phi^{k-1})}{\mathcal{D} \Phi},$$

where k indicates the iteration step for the time interval  $t \in (0,T]$  and  $\alpha$  is a parameter of descent which governs how large an update is made at each iteration, which may be adjusted at each iteration step to be that value which minimizes  $\mathcal{J}_d$ . This algorithm updates  $\Phi$  at each iteration in the direction of maximum decrease of  $\mathcal{J}_d$ . As  $k \to \infty$ , the algorithm should converge to some local minimum of  $\mathcal{J}_d$  over the control space  $\Phi$ . Note that convergence to a global minimum will not in general be attained by such a scheme, and that, as time proceeds,  $\mathcal{J}_d$  will not necessarily decrease.

Note also that the "initial" conditions in (3) are defined at t = T. The adjoint field must be marched backward in time over the interval—due to the sign of the time derivative in the adjoint operator (see Appendix), this is the natural direction for this time march. However, as  $\mathcal{A}^* = \mathcal{A}^*(U)$ , such a scheme requires storage of the flow field U on  $t \in [0, T]$ , which itself must be computed with a forward march. These storage issues are a numerical complication, but are not insurmountable.

## Relaminarization example

As in the last example, we first represent the control problem of interest as a cost functional,  $\mathcal{J}$ , to be minimized. In the present problem, control is to be applied to reduce the terminal value of turbulent kinetic energy integrated over the volume of the channel using the least amount of control effort possible. A relevant cost functional for the present problem is thus

$$\mathcal{J}_{TKE}(\Phi) = \frac{\ell}{2AT} \int_{w} \int_{0}^{T} \Phi^{2} dt dS + \frac{1}{2A} \int_{\Omega} \rho u_{i}^{\prime 2} \Big|_{t=T} dV,$$

where  $u_i'$  indicates the fluctuating velocity component. As in the previous example, the first term is a measure of the magnitude of the control, and the second term is a measure of exactly that quantity we would like to regulate—in this case, the terminal value of the turbulent kinetic energy.

The procedure to determine the gradient of the cost functional  $\mathcal{J}_{TKE}$  in the space of the control  $\Phi$  is very similar to that in the previous example. The differential change in the cost  $\mathcal{J}_{TKE}$  resulting from a differential change of the control  $\Phi$  is given by

$$\dot{\mathcal{J}}_{TKE}(\Phi) = \frac{1}{AT} \int_{w} \int_{0}^{T} \frac{\mathscr{D}\mathcal{J}_{TKE}(\Phi)}{\mathscr{D}\Phi} \dot{\Phi} dt dS 
= \frac{\ell}{AT} \int_{w} \int_{0}^{T} \Phi \dot{\Phi} dt dS 
+ \frac{1}{A} \int_{Q} \rho u_{i}' \dot{u}_{i}' \Big|_{t=T} dV,$$

where  $u_i'$  is the fluctuating velocity component of the differential state described by (2). As in the previous example, we turn to an adjoint formulation to re-express this last term.

Consider an adjoint state defined by

$$\mathcal{A}^* \tilde{U} = 0, \tag{5a}$$

with boundary conditions

$$\tilde{u}_i = 0$$
 on walls (5b)

and initial conditions

$$\tilde{u}_i = T u_i' \Big|_{t=T}$$
 at  $t = T$ , (5c)

where the adjoint operator  $\mathcal{A}^*$  is defined by the identity (4). Equation (4) may be simplified using (1), (2), and (5). The resulting expression reduces to

$$\int_{\Omega} \rho \, u_i' \, \dot{u}_i' \Big|_{t=T} \, dV = -\frac{1}{T} \int_{w} \int_{0}^{T} \tilde{p} \, \dot{\Phi} \, dt \, dS.$$

The differential of the cost functional  $\dot{\mathcal{J}}_{TKE}$  may be rewritten using this expression, which results in

$$\int_{\mathcal{W}} \int_{0}^{T} \left( \frac{\mathscr{D} \mathcal{J}_{TKE}(\Phi)}{\mathscr{D} \Phi} - \ell \, \Phi + \tilde{p} \right) \dot{\Phi} \, dt \, dS = 0.$$

Again, as  $\dot{\Phi}$  is arbitrary, this implies that

$$\frac{\mathscr{D}\mathcal{J}_{TKE}(\Phi)}{\mathscr{D}\Phi} = \ell \, \Phi - \tilde{p}.$$

Thus, the sensitivity of the cost functional  $\mathcal{J}_{TKE}$  to small changes in the control  $\Phi$  may be determined using the solution to the adjoint problem (5). An iterative control strategy may now be proposed as in the previous example to complete the control formulation.

## Results

The control formulations derived above were tested in direct numerical simulations of fully developed turbulent channel flow at Reynolds number based on shear velocity of  $Re_{\tau} = 100$ . Fourier transforms are used to compute spatial derivatives in the homogeneous directions, and a conservative second order finite difference scheme is used to compute spatial derivatives in the wallnormal direction. The computational grid is staggered in the wall-normal direction to prevent decoupling of the even and odd modes of the pressure. The flow is advanced in time using an explicit third-order Runge-Kutta method for terms involving  $x_1$  and  $x_3$  derivatives and an implicit Crank-Nicholson method for  $x_2$  derivative terms this temporal discretization is used to mitigate the time step restriction at the wall when control is applied. The number of grid points used is  $32 \times 65 \times 32$ , and the size of the computational box is  $4\pi \times 2 \times 4\pi/3$ , where  $u_{\tau} = 1$  for the uncontrolled case.

The adjoint solver is coded with a method analogous to that of the flow solver. The flow field is stored every 5 time steps on the forward sweep, with linear interpolation of these stored fields used on the backward sweep to determine  $\mathcal{A}^*$ . In the optimal calculations presented here, we chose  $\ell = 0$  (control power is taken to be "cheap"), and a simple gradient algorithm was used for the control update, with  $\alpha$  computed at each iteration by line minimization.

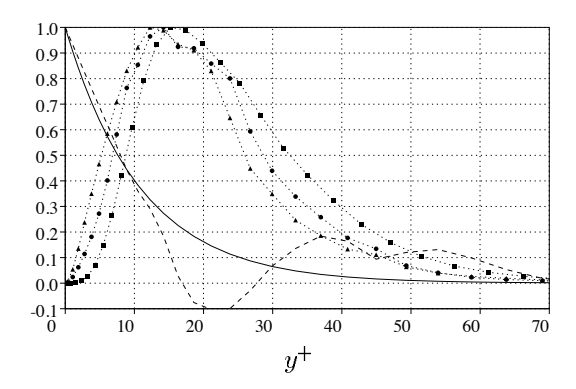


Figure 4: VARIATION OF ADJOINT QUANTITES AWAY FROM WALL FOR  $\mathcal{J}_d$  FORMULATION AT  $T^+=120$ . , spatially-averaged value of  $\tilde{u}_1$  for laminar flow; ---- , spatially-averaged value of  $\tilde{u}_1$  for turbulent flow;  $\star$  ,  $\tilde{u}_2$ (rms);  $\bullet$  ,  $\tilde{u}_1$ (rms);  $\blacksquare$  ,  $\tilde{u}_3$ (rms). Rms quantities are normalized by their peak values.

As illustrated in figure 4, an estimate of the region of maximum variation of the adjoint field for the  $\mathcal{J}_d$  formulation is  $y^+ \approx \sqrt{T^+}$ . Values of  $T^+$  which allow the adjoint field to develop into the region of interest near the coherent structures should be sought as a minimum optimization interval—given the region of interest from Choi et al. (1994) of  $y^+ = 10$ , values of  $T^+ \approx 100$  are appropriate. For values of  $T^+$  which are significantly smaller, fluctuations of the adjoint field are restricted to very near the wall, and thus flow field variations near  $y^+ = 10$  are not effectively taken into account by the adjoint field. The calculations presented below take  $T^+ = 120$ .

Figures 5a and 5b show that the drag and TKE reductions achieved by both optimal formulations presented above far exceed those of the *ad hoc* scheme illustrated in figure 2. As one would expect, the formulation for  $\mathcal{J}_d$  initially reduces the drag most effectively. Also, the formulation for  $\mathcal{J}_{TKE}$  reduces the TKE (in stages) effectively. Note that the  $\mathcal{J}_{TKE}$  formulation eventually reduces the TKE by an order of magnitude. The reduced Reynolds stresses near the wall in this case eventually result in over 50% drag reduction, which exceeds the drag reduction of the scheme designed to regulate drag directly. (As the time period T

is increased, it is believed that the disparity between these results would be reduced.)

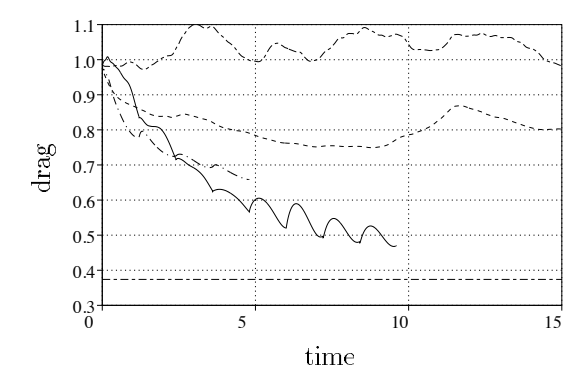


Figure 5a: DRAG HISTORY. ——, no control (upper curve is turbulent, lower curve is laminar); ———, ad hoc scheme with  $\Phi = -v (y^+ = 10)$ ; ——,  $\mathcal{J}_d$  formulation; ——,  $\mathcal{J}_{TKE}$  formulation. Optimal formulations computed with  $T^+ = 120$  and  $\ell = 0$ . Drag is normalized by mean drag in uncontrolled case, time is in units of  $\delta/u_\tau$  (uncontrolled), velocities are normalized by  $u_\tau$  (uncontrolled).

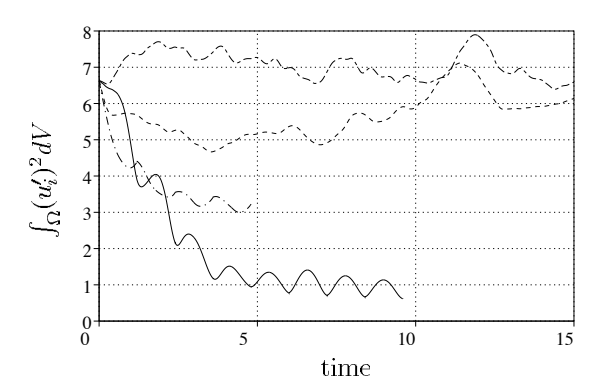


Figure 5b: TKE HISTORY. See figure 5a for explanation of plot symbols.

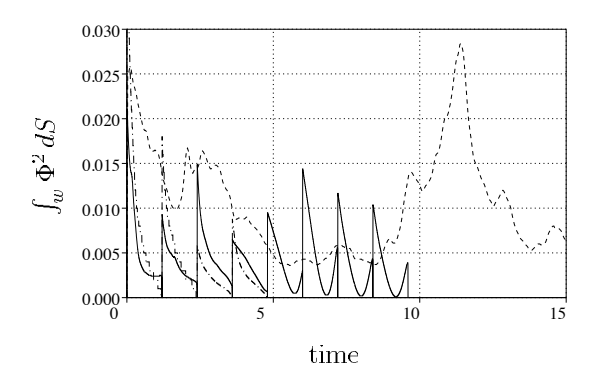


Figure 5c: CONTROL POWER HISTORY. See figure 5a for explanation of plot symbols. Time averaged values are 0.0080 for the  $ad\ hoc$  scheme, 0.0048 for the  $\mathcal{J}_d$  formulation, and 0.0042 for the  $\mathcal{J}_{TKE}$  formulation.

Figure 5c shows that these drag and TKE reductions were performed using less control power than the *ad hoc* scheme, even with the price of the control  $\ell$  set to zero in these computations. Increasing  $\ell$  resulted in smaller control levels and less effective control.

#### **IMPLEMENTATION ISSUES**

In order to be sufficiently robust, most practical feedback control sensors are flush mounted on the wall. At a wall, we may measure both skin friction (in the streamwise and spanwise directions) and wall pressure. As shown earlier in this paper, skin friction shows a fairly good correlation with near-wall coherent structures in uncontrolled flow; Choi et al. (1994) have observed that wall pressure fluctuations do not provide as good a correlation with such structures. With this limitation on flow measurement location alone, optimal control in a laboratory setting is out of reach. For this reason, three methods to reduce the optimal problem to a simple input/output relation between wall-mounted sensors and actuators are currently under investigation.

The first method is the approximate analytic solution of an approximation to the control problem. A practical feedback control rule is determined by a three step process: a) suboptimal approximation (i.e. small T), b) approximation of the near wall velocity field by an extrapolation of sensor measurements, and c) approximate solution of the resulting problem by neglecting high order products in the computation of the adjoint field. This type of rule has been successfully derived and tested and shown to give approximately 15% drag reduction in low Reynolds number turbulent channel flow (Hill 1993).

The second method is adaptive modeling of the optimal control algorithm based on sensor measurements alone. Neural networks have been shown to be effective modeling tools for flow control problems, though the training for such networks can sometimes be inefficient and slow (Goodman and Kim 1995).

The third method is to determine the coefficients in a pre-determined feedback control rule by an optimal parameter estimation technique. This method has the attractive features that it both lacks the several approximations required by method 1 to determine the control rule, while still determining the control rule directly, without stochastic modeling as required by method 2. This approach is still being formulated (Bewley 1996).

Robust actuators of the scale required for flow control create an even trickier design problem, as the actuator must interact with the flow itself, both forcefully and rapidly. The most notable advance in the past few years in the area of implementing turbulence control ideas has been the emergence of Micro Electro Mechanical Systems (MEMS) technology, which employs the methods developed for the fabrication of silicon chips to construct very small mechanical devices (Wise 1991). Miniaturization of this scale for both sensors and actuators is necessary for feedback control of turbulence due to the very small scales of the coherent structures in high Reynolds numbers flows of engineering interest (Tai 1995).

A modular configuration which is currently under investigation (Goodman et al. 1995) is to tile a portion of a wall with integrated sensor-actuatorcontroller units fabricated in silicon which can be mass-produced using MEMS technology. Estimates on the requirements for control units under flight conditions have been computed by Wilkinson (1990) and Gad-el-Hak (1994). At the typical aircraft cruise conditions quoted by Gad-el-Hak  $(u_{\infty} = 300 \text{ m/s}, u_{\tau} = 10 \text{ m/s}, \nu = 3 \cdot 10^{-5} \text{ m}^2/\text{s}),$ the wall unit scale is  $\nu/u_{\tau} = 3 \ \mu \mathrm{m}$  and the nondimensional time unit is  $\nu/u_{\tau}^2 = 0.3 \ \mu \text{sec.}$  The average spanwise spacing of the streaky structures is about 100 wall units; a few sensors and actuators must span this gap in order to effectively counter the turbulent motion, implying actuators and sensors with widths on the order of 50  $\mu$ m. The passage of coherent structures at these flight conditions (estimated by the time it takes a coherent structure to convect at  $0.8u_{\infty}$  a distance of 400 wall units) would be approximately once every 5  $\mu$ sec. Power requirements have been considered by Muntz et al. (1993). These guidelines give very rough estimates on the spatial density of sensors and actuators and the response time required in their implementation—production of control units on this scale with today's technology would be difficult.

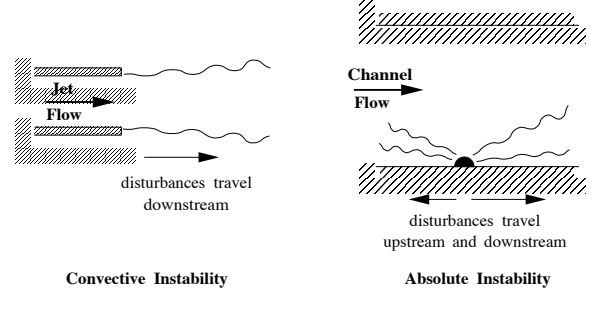


Figure 6. TWO TYPES OF FLOW INSTABILITY.

Linear stability theory (Drazin and Reid 1981) can be quite useful when considering flow control problems. In some flow configurations, as shown in figure 6, all growing disturbances convect downstream from their source, in which case

the flow is said to be convectively unstable. This is in contrast to the case in which some of the growing disturbances can travel back upstream and continually disrupt the flow even after the initial disturbance is neutralized, which is referred to as absolute instability (Huerre and Monkewitz 1985). In configurations which are convectively unstable, active control schemes applied near the point where perturbations originate can be especially effective. For example, the effects of a control scheme can be quite dramatic when applied near the transition point of a boundary layer flow, the separation point on an airfoil, or the nozzle of a jet, where flow instabilities magnify quickly. It is on such critical flow regimes that our attention should focus as we attempt to implement feedback flow control in the years to come.

#### **ACKNOWLEDGEMENTS**

The authors are grateful for close collaborations with Prof. Roger Temam, whose guidance was crucial for the theoretical aspect of this work. Mr. Artur Kravchenko is also acknowledged for help in preparing this document. The financial support of AFOSR Grant No. F49620-93-1-0078 is also gratefully acknowledged.

## **REFERENCES**

- ABERGEL, F & TEMAM, R 1990 On some control problems in fluid mechanics. *Theor. and Comp. Fluid Dynamics.* 1, 303.
- BECHERT, DW & BARTENWERFER, M 1989 The viscous flow on surfaces with longitudinal ribs. *J. Fluid Mech.*. **206**, 105.
- Bewley, T 1996 Optimal feedback control of turbulence. Ph.D. Thesis (in preparation), Department of Mechanical Engineering, Stanford University.
- Blackwelder, RF 1989 Some ideas on the control of near-wall eddies. AIAA Paper No. 89-1009.
- Bushnell, DM & McGinley, CB 1989 Turbulence control in wall flows. *Ann. Rev. Fluid Mech.*. 21, 1.
- CANTWELL, BJ 1981 Organized motion in turbulent flow. Annu. Rev. Fluid Mech.. 13, 437.
- Choi, H, Moin, P, & Kim, J 1993 Direct numerical simulation of turbulent flow over riblets. J. Fluid Mech.. 255, 503.
- CHOI, H, MOIN, P, & KIM, J 1994 Active turbulence control for drag reduction in wall-bounded flows. J. Fluid Mech. 262, 75.
- DRAZIN, PG, & REID, WH 1981 Hydrodynamic Stability, Cambridge University Press, London.
- FIEDLER, HE & FERNHOLZ, HH 1990 On management and control of turbulent shear flows. *Prog. Aerospace Sci..* 27, 305.

- GAD-EL-HAK, M 1989 Flow Control. *Appl. Mech. Rev.*. **42**, (10).
- GAD-EL-HAK, M 1994 Interactive control of turbulent boundary layers: a futuristic overview. AIAA J. 32, (9), 1753.
- GOODMAN, R et al. 1995 Integrated Vortex Control by MEMS Based Transducers, presented at the AFOSR Contractor and Grantee Meeting on Turbulence and Internal Flows, Wright Patterson AFB, May 15, 1995.
- GOODMAN, R, & KIM, J 1995 Application of Neural Networks to Flow Control, presented at the AFOSR Contractor and Grantee Meeting on Turbulence and Internal Flows, Wright Patterson AFB, May 15, 1995.
- HUERRE, P, & MONKEWITZ, PA 1985 Absolute and convective instabilities in free shear layers. J. Fluid Mech. 159, 151.
- HILL, DC 1993 Drag reduction at a plane wall. Annual Research Briefs-1993, Center for Turbulence Research, Stanford U./NASA Ames.
- KRAVCHENKO, AG, CHOI, H, & MOIN, P 1993 On the relation of near-wall steamwise vortices to wall skin friction in turbulent boundary layers. *Phys. Fluids A.* **5**, (12), 3307.
- LEE, M & REYNOLDS, WC 1985 Bifurcating and blooming jets, Rept TF-22, Thermo Sciences Division, Dept of Mech Eng, Stanford University.
- LIONS, JL 1968 Controle Optimal des Systèmes Gouvernés par des Equations aux Dérivées Partielles. Dunod, Paris. English translation, Springer-Verlag, New York.
- Moin, P, & Bewley, T 1994 Feedback control of turbulence. *Appl. Mech. Rev.*. 47, (6), part 2.
- MUNTZ, EP, SHIFLETT, GR, WADSWORTH, D, & BLACKWELDER, RF 1993 Transient energy release pressure driven microactuators for flow control. AIAA Paper No. 93-3271.
- NOSENCHUCK, D, & BROWN, G 1993 Control of turbulent wall shear stress using arrays of TFM tiles. Bull. Am. Phys. Soc.. 38, (12), 2197.
- Padmanabhan, KT, Bowman, CT, & Pow-Ell, JD 1993 Development of an adaptive optimal combustion control strategy. *The Combustion Institute Paper No. 93-092.*
- RILEY, JJ, GAD-EL-HAK, M, & METCALFE, RW 1988 Compliant Coatings. Ann. Rev. Fluid Mech.. 20, 393.
- ROBINSON, SK 1991 Coherent motions in the turbulent boundary layer. Ann. Rev. Fluid Mech.. 23, 601.
- TAI, YC 1995 Micro Sensors and Micro Actuators, presented at the AFOSR Contractor and Grantee Meeting on Turbulence and Internal Flows, Wright Patterson AFB, May 15, 1995.
- VAINBERG, M 1964 Variational Methods for the Study of Nonlinear Operators. Holden-Day, p 54.
- WALSH, MJ 1990 Riblets, in Viscous drag reduction in boundary layers, eds. Bushnell, DM and

Hefner, JN, *Progress in Astro and Aeronautics* **123**, 203-261, AIAA, Washington, DC.

WILKINSON, SP 1990 Interactive wall turbulence control, in Viscous drag reduction in boundary layers, eds. Bushnell, DM and Hefner, JN, Progress in Astro and Aeronautics 123, 479-509, AIAA, Washington, DC.

WISE, KD 1991 Integrated microelectromechanical systems: a perspective on MEMS in the 90s. *Proc* 1991 IEEE MEMS Workshop, 33.

# **APPENDIX**

The fields referred to in this work are the flow field U, the differential field  $\dot{U}$ , and the adjoint field  $\tilde{U}$ , each of which is broken into three velocity components and a pressure component

$$U = \begin{pmatrix} u_i(x_1, x_2, x_3, t) \\ p(x_1, x_2, x_3, t) \end{pmatrix}, \quad \dot{U} = \begin{pmatrix} \dot{u}_i(x_1, x_2, x_3, t) \\ \dot{p}(x_1, x_2, x_3, t) \end{pmatrix}, \quad \tilde{U} = \begin{pmatrix} \tilde{u}_i(x_1, x_2, x_3, t) \\ \tilde{p}(x_1, x_2, x_3, t) \end{pmatrix}.$$

The Navier-Stokes operator is given by

$$\mathcal{N}(U) = \begin{pmatrix} \frac{\partial u_i}{\partial t} + u_j \frac{\partial u_i}{\partial x_j} - \nu \frac{\partial^2 u_i}{\partial x_j^2} + \frac{1}{\rho} \frac{\partial p}{\partial x_i} + \frac{1}{\rho} \delta_{1i} P_x \\ \frac{\partial u_j}{\partial x_i} \end{pmatrix}.$$

Consider the Fréchet differential (Vainberg, 1964) of the flow U and the cost  $\mathcal{J}$ :

$$\dot{U} \equiv \frac{1}{AT} \lim_{\epsilon \to 0} \frac{U(\Phi + \epsilon \dot{\Phi}) - U(\Phi)}{\epsilon} = \frac{1}{AT} \int_{w} \int_{0}^{T} \frac{\mathscr{D}U(\Phi)}{\mathscr{D}\Phi} \dot{\Phi} \, dt \, dS$$

$$\dot{\mathcal{J}} \equiv \frac{1}{AT} \lim_{\epsilon \to 0} \frac{\mathcal{J}(\Phi + \epsilon \dot{\Phi}) - \mathcal{J}(\Phi)}{\epsilon} = \frac{1}{AT} \int_{w} \int_{0}^{T} \frac{\mathscr{D}\mathcal{J}(\Phi)}{\mathscr{D}\Phi} \dot{\Phi} dt dS,$$

where  $\dot{\Phi}$  is an arbitrary control update direction, which will remain undetermined and will later be isolated and removed from the equation for the differential of the cost functional. The Fréchet differential of the (non-linear) Navier-Stokes operator is given by

$$\label{eq:delta} \mathcal{A}\dot{U} = \left( \begin{array}{c} \frac{\partial \dot{u}_i}{\partial t} + u_j \frac{\partial \dot{u}_i}{\partial x_j} + \dot{u}_j \frac{\partial u_i}{\partial x_j} - \nu \frac{\partial^2 \dot{u}_i}{\partial x_j^2} + \frac{1}{\rho} \frac{\partial \dot{p}}{\partial x_i} \\ \\ -\frac{1}{\rho} \frac{\partial \dot{u}_j}{\partial x_i} \end{array} \right),$$

which is linear in the differential field  $\dot{U}$ , but is a function of the solution U of the Navier-Stokes problem, so that  $\mathcal{A} = \mathcal{A}(U)$ . Define an inner product over the domain in space-time under consideration such that

$$<\dot{U}, \tilde{U}> = \int_{\Omega} \int_{0}^{T} \dot{U} \cdot \tilde{U} dt dV,$$

and consider the defining identity

$$\langle \mathcal{A}\dot{U}, \tilde{U} \rangle = \langle \dot{U}, \mathcal{A}^*\tilde{U} \rangle + b.$$
 (6)

Integration by parts may be used to move all differential operations from  $\dot{U}$  on the left hand side of the equation to  $\tilde{U}$  on the right hand side, resulting in an expression for the adjoint operator

$$\mathcal{A}^* \tilde{U} = \begin{pmatrix} -\frac{\partial \tilde{u}_i}{\partial t} - u_j \left( \frac{\partial \tilde{u}_i}{\partial x_j} + \frac{\partial \tilde{u}_j}{\partial x_i} \right) - \nu \frac{\partial^2 \tilde{u}_i}{\partial x_j^2} + \frac{1}{\rho} \frac{\partial \tilde{p}}{\partial x_i} \\ -\frac{1}{\rho} \frac{\partial \tilde{u}_j}{\partial x_j} \end{pmatrix},$$

where  $A^* = A^*(U)$ , and an expression for b, which contains all the boundary terms:

$$b = \int_{w} \int_{0}^{T} -n_{j} \left( \tilde{u}_{i} \left( u_{j} \, \dot{u}_{i} + u_{i} \, \dot{u}_{j} \right) - \nu \left( \frac{\partial \dot{u}_{i}}{\partial x_{j}} \, \tilde{u}_{i} - \dot{u}_{i} \, \frac{\partial \tilde{u}_{i}}{\partial x_{j}} \right) + \frac{1}{\rho} \left( \dot{p} \, \tilde{u}_{j} - \dot{u}_{j} \, \tilde{p} \right) \right) dt \, dS$$
$$+ \int_{\Omega} \dot{u}_{i} \, \tilde{u}_{i} \, dV \Big|_{t=T} - \int_{\Omega} \dot{u}_{i} \, \tilde{u}_{i} \, dV \Big|_{t=0}.$$

Simplification of the identity (6) by interior equations, boundary conditions, and initial conditions on U,  $\dot{U}$ , and  $\tilde{U}$  can provide an expression which recasts  $\dot{\mathcal{J}}$  from a (difficult to determine) function of  $\dot{U}$  to a more manageable function of the solution to an adjoint problem for  $\tilde{U}$ .